




Optimization of luminescence properties of Tb³⁺-doped α -Sr₂P₂O₇ phosphor synthesized by combustion method

Nimesh Prafulbhai Patel* , Mangalampalli Srinivas,
Dhaval Modi, Vishwnath Verma, Kota Venkata Ramana Murthy

Received: 6 July 2015/Revised: 28 August 2015/Accepted: 18 December 2015/Published online: 12 January 2016
© The Nonferrous Metals Society of China and Springer-Verlag Berlin Heidelberg 2016

Abstract In this paper, thermoluminescence (TL) properties of rare earth Tb³⁺-doped α -Sr₂P₂O₇ were examined after β -irradiation and photoluminescence (PL) properties of samples were examined for proper excitation. All the samples were synthesized by high-temperature combustion method. The X-ray diffraction (XRD) and Fourier transform infrared (FTIR) spectroscopy characterization confirms the formation of pure α -phase with crystallized in orthorhombic structure of samples. The PL emission spectra of all samples exhibit characteristic green emission peaks of Tb³⁺ where the peak at 545 nm has the highest emission intensity for Tb³⁺ concentration of 5.0 mol%. The TL glow curves of β -irradiated Tb³⁺-doped α -Sr₂P₂O₇ phosphors were recorded at different heating rates of 2, 4, and 6 K·s⁻¹. TL curves of all sample exhibit combination of two peaks: peak at 420 K shifts toward higher temperature, while peak at 525 K remains unaffected with the increase in Tb³⁺ concentration as well as fading effect. The activation energy and kinetic parameters of the samples were evaluated using thermoluminescence peak shape method.

Keywords Rare earth doping; Strontium pyrophosphate; β -Irradiation; Photoluminescence; Thermoluminescence

1 Introduction

Pyrophosphate-based materials are scientifically important because of their luminescent, dielectric, semiconducting, catalytic, magnetic, fluorescent, and ion-exchange properties. Because of remarkable properties, the synthesis of inorganic pyrophosphate materials is a dynamic field of research, especially in luminescence aspects [1–10]. The thermoluminescence (TL) dosimetry properties of Sr₂P₂O₇:Cu, Pr compounds have been studied [1]. In previous work, photoluminescence (PL) and dosimetry properties of Ce-activated α -Sr₂P₂O₇ phosphor were synthesized by a high-temperature combustion method and X-ray-irradiated TL properties of Dy³⁺-doped α -Sr₂P₂O₇ were studied [2, 3]. Eu²⁺- and Mn²⁺-co-doped Sr₂P₂O₇ phosphors were suggested as the potential phosphors for obtaining white-light emission from ultraviolet-light-emitting diode (UV-LED) devices [4].

The TL properties of pure and doped strontium pyrophosphates were widely examined, because the rare earth activated inorganic phosphors are extensively used in a variety of applications in lamp phosphors, color displays, radiation dosimetry, and X-ray imaging [5]. Singly and doubly doped strontium phosphate α -Sr(PO₃)₂ was compared with equivalently doped diphosphates α -Sr₂(P₂O₇) and SrZn(P₂O₇), and the crystal structure determination of SrZn(P₂O₇) based on single-crystal data was evaluated [6]. Eu²⁺-activated SrCaP₂O₇ phosphor was suggested as blue-emitting phosphor [7]. Alkaline earth metal pyrophosphates M₂P₂O₇ (M = Ca, Sr, Ba) were proposed for their potential applications as luminescent materials, for

N. P. Patel*, M. Srinivas, D. Modi, V. Verma
Luminescence Material Laboratory, Department of Physics,
Faculty of Science, The M. S. University of Baroda, Vadodara
390002, India
e-mail: nimesh.0112@gmail.com

K. V. R. Murthy
Display Materials Laboratory, Applied Physics Department,
Faculty of Technology and Engineering, The M. S. University of
Baroda, Vadodara 390001, India

example, $\text{Sr}_2\text{P}_2\text{O}_7:\text{Eu}^{3+}$, Tb^{3+} ; $\text{Ca}_2\text{P}_2\text{O}_7:\text{Eu}^{2+}$, Y^{3+} ; $\text{Sr}_2\text{P}_2\text{O}_7:\text{Eu}^{2+}$, Mn^{2+} ; $\text{Ca}_2\text{P}_2\text{O}_7:\text{Eu}^{2+}$, Mn^{2+} [8–10].

In this paper, PL property of phosphor was examined for various Tb^{3+} concentrations and the TL property of Tb^{3+} -activated $\alpha\text{-Sr}_2\text{P}_2\text{O}_7$ was explained on the basis of fading effect. The activation energy, frequency factors, and order of kinetics of the glow curves were calculated by peak shape method with curve fitting information. PL studies suggest the phosphor as excellent green phosphor and TL of phosphor is also quite good important.

2 Experimental

Tb^{3+} -doped $\text{Sr}_2\text{P}_2\text{O}_7$ phosphors were synthesized by high-temperature combustion method. The samples with various Tb^{3+} concentrations (0.5 mol%, 1.0 mol%, 1.5 mol%, 2.0 mol%, 2.5 mol% and 5.0 mol%) were synthesized. The starting reactants SrCO_3 , $(\text{NH}_4)_2\text{HPO}_4$ and Tb_4O_7 (99.99 %) (all in analytical reagent (AR)) were taken as per stoichiometric proportion and grinded in an agate mortar with urea (AR; 15 wt% of the mixture) to make homogeneous mixture. Urea was taken as a flux in this method to raise the combustion process. The grinded mixture was placed in an alumina crucible and heated at 1200 °C for 3 h in a muffle furnace in air and then naturally cooled down to room temperature. The sample in the form of pure white fine powder was obtained after grinding the product [2, 3].

The prepared samples were first characterized by X-ray diffractometer (XRD, Bruker D8; Cu $\text{K}\alpha$ radiation, $\lambda = 0.15406$ nm, 40 kV and 40 mA) to examine crystal phase formation and structural parameters of phosphors. The XRD measurements were carried out for glancing angle incidence detector at an angle of 2° for 2θ values of 10°–60° in steps of 0.02°. Fourier transform infrared (FTIR) spectra of the samples were recorded by FTIR-4100 type A IR spectrometer in transmittance mode in wavenumber range of 400–4000 cm^{-1} . The PL properties of the phosphor were examined using a Shimadzu spectrofluorometer (1503 R-PC). PL excitation and emission spectra were recorded by a xenon lamp through a monochromator. The TL glow curves of β -irradiated samples were taken using a NUCLEONIX TL analyzer type TL1009 at different heating rates (β) of 2, 4, and 6 $\text{K}\cdot\text{s}^{-1}$.

3 Theory

The activation energy (E_a), frequency factor (s), and order of kinetics (b) of glow curves were calculated using Chen's peak shape method [11]. Chen's method had functional application with a broad energy range between 0.1 and 2.0 eV and the pre-exponential factor (frequency factor) of

1×10^5 – $1 \times 10^{23} \text{ s}^{-1}$. For analysis of activation energy by Chen's method, necessary information of the kinetic order is not required. The geometric factor (μ_g) was calculated to determine the order of kinetics of glow curve. In this method, three equations for first- and second-order kinetics are derived correlated with the trap depth: a full width of the peak at half maximum ($\omega = T_2 - T_1$), a low-temperature half width ($\tau = T_m - T_1$), and a high-temperature half width ($\delta = T_2 - T_m$), where T_1 and T_2 are low and high temperatures corresponding to half-maximum intensity, respectively; and T_m is the peak temperature at maximum intensity.

The general equation for evaluating activation energy (E_a) is given as:

$$E_a(\gamma) = c_\gamma \left(\frac{kT_m^2}{\gamma} \right) - b_\gamma(2kT_m) \quad (1)$$

where k is the Boltzmann's constant, $\gamma = \tau, \delta, \omega$, and c_γ and b_γ are constants which can be calculated using following formula:

$$c_\tau = 1.51 + 3(\mu_g - 0.42) \quad (2)$$

$$c_\delta = 0.976 + 7.3(\mu_g - 0.42) \quad (3)$$

$$c_\omega = 2.52 + 10.2(\mu_g - 0.42) \quad (4)$$

$$b_\tau = 1.58 + 4.2(\mu_g - 0.42) \quad (5)$$

$$b_\delta = 0 \quad (6)$$

$$b_\omega = 0 \quad (7)$$

$$\mu_g = \frac{\delta}{\omega} \quad (8)$$

Peak shape method is also very useful for estimating the order of kinetics of the TL peaks. As per this method, the order of kinetics (b) was determined by the geometric shape factor (μ_g). In general, suggested values of geometric factor are $\mu_g = 0.42$ for the first-order kinetics and $\mu_g = 0.52$ for the second-order kinetics [11–13].

4 Results and discussion

4.1 XRD analysis

Figure 1 shows XRD patterns of $\text{Sr}_2\text{P}_2\text{O}_7$ phosphors doped with Tb^{3+} concentrations of 0.5 mol%, 2.5 mol%, and 5.0 mol%. The XRD patterns illustrate that the structural formation of all samples are very similar to that of the of $\alpha\text{-Sr}_2\text{P}_2\text{O}_7$ (JCPDS No. 24-1011), in which $\text{Sr}_2\text{P}_2\text{O}_7$ has an α -phase orthorhombic crystal structure with $Pnam$ space group (JCPDS No. 24-1011). The doping of Tb^{3+} does not show any measurable influence on the host structure [2, 3, 14, 15]. Tb^{3+} cannot replace P^{5+} , but it can easily fit into the site of Sr^{3+} as

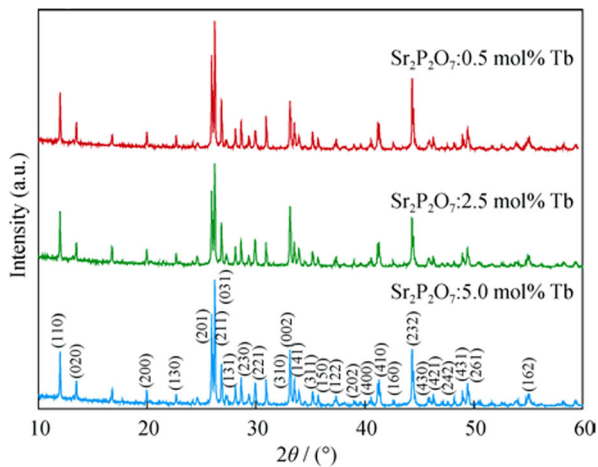


Fig. 1 XRD patterns of Tb-doped Sr₂P₂O₇ phosphors

the ionic radius of Tb³⁺ (0.0923 nm) is smaller than that of Sr²⁺ (0.114 nm) and larger than that of P⁵⁺ (0.052 nm) [16]. Lattice constants of Sr₂P₂O₇:2.5 mol% Tb calculated are $a = 0.8865$ nm, $b = 1.3142$ nm, $c = 0.5421$ nm, $V = 0.631567$ nm³ and $\alpha = \beta = \gamma = 90^\circ$. The lattice parameters obtained with different Tb³⁺ concentrations show very similar nature and the XRD results of Tb³⁺-doped samples are quite consistent with previous work [2, 3].

4.2 FTIR results

FTIR transmittance spectra of Tb³⁺-doped Sr₂P₂O₇ were recorded using KBr pellets. KBr pellet of all samples were prepared in a 99:1 weight ratio of KBr to Sr₂P₂O₇ for total weight at a thickness of 1 mm. Figure 2 shows FTIR spectra of Tb³⁺-doped Sr₂P₂O₇ phosphors in the wavenumber range of 400–2000 cm⁻¹. The FTIR spectra show characteristic absorption bands of pyrophosphate group (P₂O₇)⁻⁴ at 746 and 1190 cm⁻¹, which explain the formation of pyrophosphate groups [2, 3]. Peak observed at

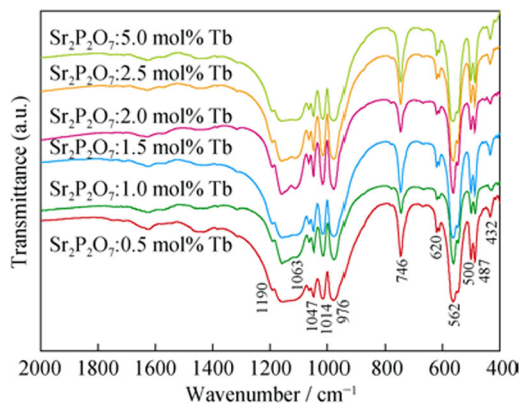


Fig. 2 FTIR spectra of Tb³⁺-doped Sr₂P₂O₇ phosphors

1047 cm⁻¹ is attributed to the antisymmetric stretching mode of (P–O)_{v3}. Broad peak located at 976 cm⁻¹ is attributed to the symmetric stretching mode of (P–O)_{v1}. The solder peaks at 620 cm⁻¹ is ascribed the bending mode of (O–P–O)_{v4} [2, 3, 17]. The peaks observed in the range of 450–750 cm⁻¹ correspond to the antisymmetric bending modes of PO₄, while the peaks between 950 and 1200 cm⁻¹ are attributed to the stretching modes of PO₄ [2, 3, 18]. FTIR peaks located at 976, 1014, 1047, 1062, and 1109 cm⁻¹ are attributed to the antisymmetric stretching mode of P–O bond of (PO₄)⁻³ groups in Sr₂P₂O₇ [2, 3]. The bands at 547, 562, 612, and 620 cm⁻¹ are assigned to the antisymmetric bending vibration of (PO₄)⁻³ groups [18–20]. The FTIR spectra show that the positions of all the peaks remain unaffected for various Tb³⁺ doping concentrations. Thus, the doping of Tb³⁺ does not affect the bond structure formation of host Sr₂P₂O₇, which is very similar to that of XRD observations.

4.3 PL properties

Figure 3a shows excitation spectrum of Tb³⁺-doped α -Sr₂P₂O₇ phosphor monitored at 545-nm emission wavelength. The excitation spectra exhibits a single band peaked at 232 nm due to the 4f⁸–4f⁷5d¹ (f–d) transition of Tb³⁺. An excitation band illustrates that the phosphor can be excited through the UV light of about 232 nm. Figure 3b illustrates the PL emission spectra, recorded by exciting the samples at their optimized excitation wavelength (i.e., 232 nm) to determine the PL emission from samples. It is important to find out the detailed information of the nature of the Tb³⁺ luminescence center formed inside host lattice. The emission spectra do not give all information about luminescence center, due to the high degeneracy of the Tb³⁺ levels involved in several transitions.

The PL emission spectra of the Tb³⁺-doped α -Sr₂P₂O₇ show peaks at 415, 436, 469, 491, 545 and 584 nm as a consequence of the characteristics radiative transitions of Tb³⁺. All defined transitions occurring correspond to the ⁵D₃–⁷F₅, ⁵D₃–⁷F₄, ⁵D₃–⁷F₃, ⁵D₄–⁷F₆, ⁵D₄–⁷F₅, and ⁵D₄–⁷F₄, respectively. The observed high intense peak at 545 nm can be attributed to green emission which is a characteristic emission of Tb³⁺. Tb³⁺ replaces the host Sr²⁺ from lattice site without any structural deformation, which is mainly responsible for contraction of unit cell of host Sr₂P₂O₇. The doping ions occupy the host lattice site and create metastable states inside the energy gap of host, which is the reason for the occurrence of PL emissions. It is inferred that the energy transfer process occurs between host (Sr₂P₂O₇) and activator Tb³⁺, and a very strong green emission occurs at 545 nm because of ⁵D₄–⁷F₅ electronic transition.

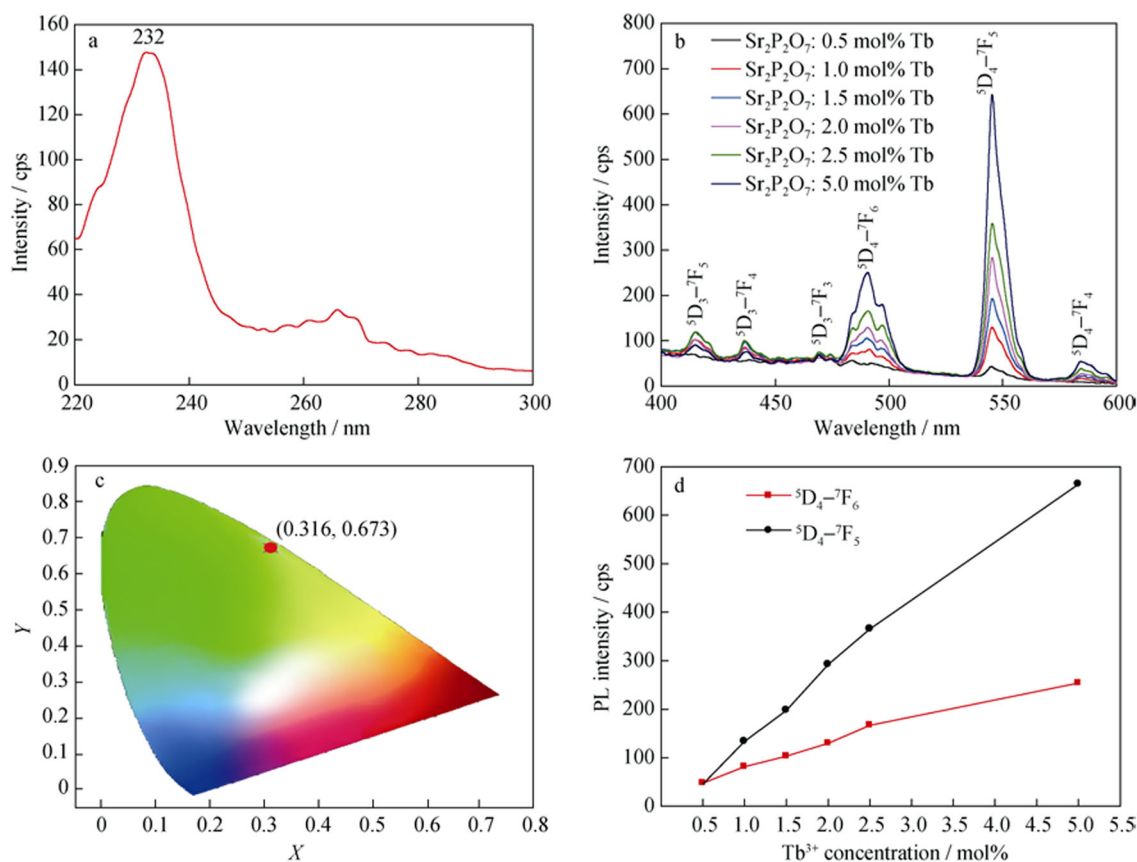


Fig. 3 Excitation spectra of Tb³⁺-doped α-Sr₂P₂O₇ recorded at emission wavelength of 545 nm **a**, PL excitation spectra of Tb³⁺-doped α-Sr₂P₂O₇ recorded at excitation wavelength of 232 nm **b**, International Commission on Illumination CIE (Commission internationale de l'éclairage) coordinates of Tb³⁺-doped α-Sr₂P₂O₇ phosphors **c**, and effect of doping Tb³⁺ concentration on emission intensity of host α-Sr₂P₂O₇ **d**

Tb³⁺ doping ion is effectively observed through the characteristic emission lines, where the emission intensity is lower for small Tb³⁺ concentrations, indicating that the dopant can be clustered or incorporated onto the lattice sites of host α-Sr₂P₂O₇. The chromaticity coordinates of PL emission spectra recorded at 232-nm excitation are shown in Fig. 3c. The chromaticity coordinates of Tb³⁺-doped α-Sr₂P₂O₇ phosphor are $X = 0.316$, $Y = 0.673$, which are falling into the green region in the chromaticity diagram and remain the same for all Tb³⁺ concentrations. Figure 3d exhibits the variation of intensity for two dominant transitions ⁵D₄-⁷F₆ and ⁵D₄-⁷F₅ with various Tb³⁺ doping concentrations. The intensity of emission occurred due to ⁵D₄-⁷F₅ transition is 2–3 times higher than that of ⁵D₄-⁷F₆ transition. Concentration quenching effect of doping was not studied, but the green emission could be optimized for 5 mol% Tb³⁺.

4.4 TL properties

Figure 4 shows the TL glow curves fitted by deconvolution method for α-Sr₂P₂O₇:0.5 mol% Tb, to formulate the trap

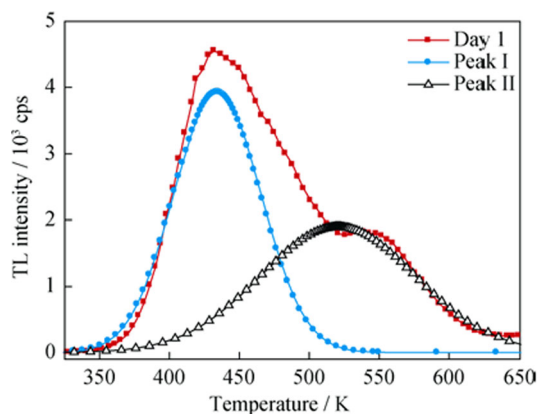


Fig. 4 Glow curves fitting of α-Sr₂P₂O₇:0.5 mol% Tb³⁺ recorded at heating rate of 6 K·s⁻¹

depth created inside the band structure of α-Sr₂P₂O₇ phosphors by doping Tb³⁺. All the samples were irradiated for a dose of 10 J·kg⁻¹ using Sr⁹⁰ β-source. The fading effect after β-irradiation on glow curves of all Tb³⁺-doped α-Sr₂P₂O₇ samples recorded at a heating rate of 6 K·s⁻¹ are

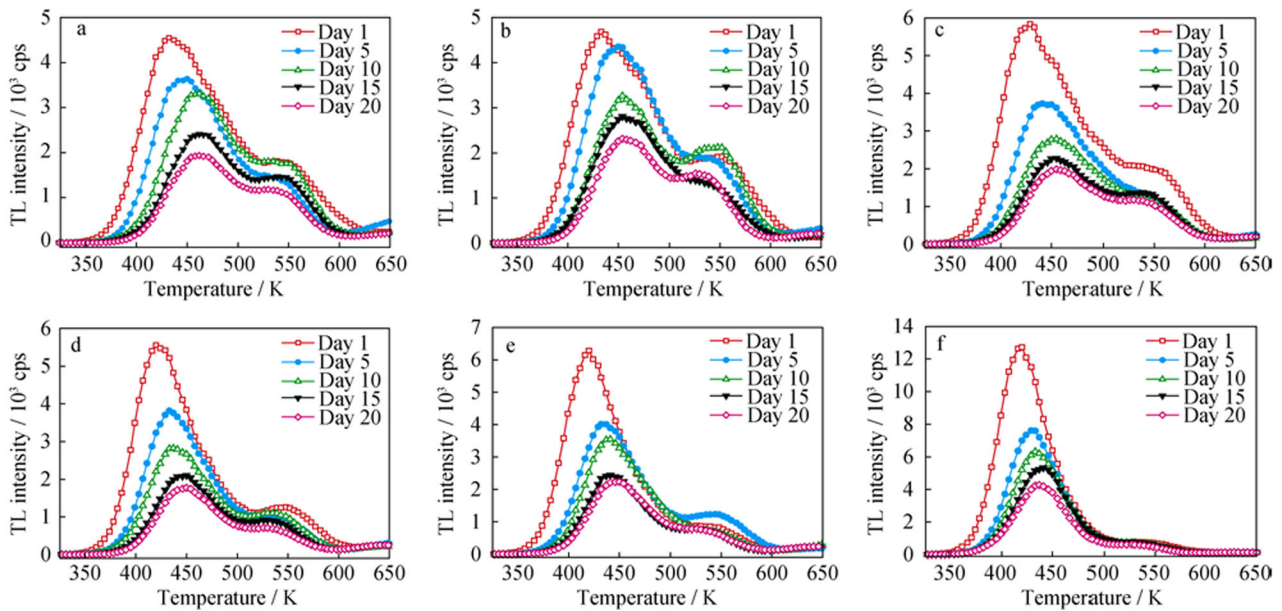


Fig. 5 Fading effect on glow curves of Tb³⁺-doped α -Sr₂P₂O₇ recorded at heating rate of 6 K·s⁻¹: **a** Sr₂P₂O₇:0.5 mol% Tb, **b** Sr₂P₂O₇:1.0 mol% Tb, **c** Sr₂P₂O₇:1.5 mol% Tb, **d** Sr₂P₂O₇:2.0 mol% Tb, **e** Sr₂P₂O₇:2.5 mol% Tb, and **f** Sr₂P₂O₇:5.0 mol% Tb

depicted in Fig. 5. The glow curves for various Tb³⁺ concentrations demonstrate that the intensity of TL glow curve decreases from Day 1 to Day 20, in which the peak temperature of the first peak at 420 K shifts toward higher temperature, while that of the second peak at 525 K remains unaffected. It is also observed that at highest Tb³⁺ concentration (5.0 mol%), the second peak at 525 K of glow curve almost vanishes due to energy transfer process; therefore, the intensity of the first peak increases dominantly. TL glow curves analysis were done by Chen's peak shape method by evaluating order of kinetics (*b*) and activation energy (*E_a*) recorded at a different heating rates of 2, 4, and 6 K·s⁻¹, and the glow curves were fitted by deconvolution method. From the curve fitting method, it is found that the glow curve consists of two peaks, the first peak is centered at around 420–435 K, and the second peak is centered at around 525 K.

All estimated parameters like energy of trap depths (activation energy) (*E_a*), order of kinetics (*b*), and frequency factor (*s*) at different heating rates are mentioned in Table 1. The energy of trap depth for the first fitted curve peaked at 420 K is around 0.8–0.9 eV and that of the second fitted curve peaked at 525 K is around 0.5–0.6 eV. The calculated values of frequency factor (*s*) are around 1×10^6 – 1×10^{11} s⁻¹, which is very small compared to that of the expected lattice vibration of 1×10^{12} – 1×10^{14} s⁻¹ [21]. The observed low-frequency factor is a characteristic of localized transitions in which radiative recombination process can take place without the involvement of a transition

of the electrons from conduction band to the valence band. Low activation energy indicates that the probability of localized detrapping process occurs due to the doping of Tb³⁺, radiative localized transitions, and the extent of wave function overlaps between the trap and the recombination center [22, 23]. TL property of the Tb³⁺-doped Sr₂P₂O₇ phosphors is mainly due to the defect centers created by substitution of Sr²⁺ by Tb³⁺ which does not affect the structure of α -Sr₂P₂O₇. TL sensitivity of α -Sr₂P₂O₇:Tb³⁺ phosphor predominantly depends on Tb³⁺ concentration, and optimum concentration is observed to be 5.0 mol% in Fig. 5. The geometric factor estimated from TL analysis is around $\mu_g = 0.50$ – 0.52 for both peaks, which is nearer to that of Chen's suggested value $\mu_g = 0.52$ for the second-order kinetics.

Figure 6 shows the variation in activation energy (*E_a*) with different Tb³⁺ doping concentrations. The activation energies of TL glow curve calculated for both peaks for the different doping concentrations are significantly uniform. The results indicate that the same TL mechanism occurs in all samples, revealing that the phosphor could be good for thermoluminescence dosimeter (TLD).

5 Conclusion

Tb³⁺-doped α -Sr₂P₂O₇ phosphors were synthesized by high-temperature combustion method using urea as a flux. XRD and FTIR studies confirm that the host has

Table 1 Activation energy, frequency factor, and order of kinetic calculated using peak shape method

Samples	$\beta/(\text{K}\cdot\text{s}^{-1})$	Curves	μ_g	$E_a(\tau)/\text{eV}$	$E_a(\delta)/\text{eV}$	$E_a(\omega)/\text{eV}$	s/s^{-1}	b
Sr ₂ P ₂ O ₇ :0.5 mol% Tb	2	Curve 1	0.51	0.81 ± 0.04	0.83 ± 0.04	0.82 ± 0.03	1.3 × 10 ⁹	2
		Curve 2	0.50	0.52 ± 0.03	0.57 ± 0.01	0.53 ± 0.02	1.6 × 10 ⁶	2
	4	Curve 1	0.51	0.82 ± 0.03	0.87 ± 0.03	0.85 ± 0.04	2.1 × 10 ⁹	2
		Curve 2	0.50	0.53 ± 0.04	0.51 ± 0.05	0.57 ± 0.03	3.4 × 10 ⁶	2
	6	Curve 1	0.51	0.81 ± 0.03	0.87 ± 0.04	0.84 ± 0.04	4.5 × 10 ⁹	2
		Curve 2	0.50	0.55 ± 0.02	0.55 ± 0.03	0.52 ± 0.02	6.2 × 10 ⁶	2
Sr ₂ P ₂ O ₇ :1.0 mol% Tb	2	Curve 1	0.52	0.80 ± 0.04	0.83 ± 0.03	0.82 ± 0.02	2.7 × 10 ⁹	2
		Curve 2	0.50	0.51 ± 0.03	0.60 ± 0.02	0.55 ± 0.02	4.5 × 10 ⁶	2
	4	Curve 1	0.52	0.83 ± 0.02	0.88 ± 0.03	0.86 ± 0.03	4.4 × 10 ⁹	2
		Curve 2	0.50	0.58 ± 0.04	0.56 ± 0.04	0.57 ± 0.03	5.1 × 10 ⁶	2
	6	Curve 1	0.52	0.84 ± 0.03	0.86 ± 0.03	0.87 ± 0.04	6.9 × 10 ⁹	2
		Curve 2	0.50	0.55 ± 0.02	0.54 ± 0.03	0.51 ± 0.03	8.9 × 10 ⁶	2
Sr ₂ P ₂ O ₇ :1.5 mol% Tb	2	Curve 1	0.52	0.83 ± 0.03	0.82 ± 0.03	0.81 ± 0.04	5.4 × 10 ⁹	2
		Curve 2	0.51	0.55 ± 0.03	0.60 ± 0.04	0.55 ± 0.04	5.8 × 10 ⁶	2
	4	Curve 1	0.52	0.85 ± 0.04	0.89 ± 0.02	0.87 ± 0.02	7.3 × 10 ⁹	2
		Curve 2	0.51	0.56 ± 0.02	0.59 ± 0.03	0.55 ± 0.04	7.6 × 10 ⁶	2
	6	Curve 1	0.52	0.88 ± 0.02	0.89 ± 0.04	0.89 ± 0.03	8.8 × 10 ¹⁰	2
		Curve 2	0.51	0.54 ± 0.04	0.56 ± 0.04	0.54 ± 0.04	1.1 × 10 ⁷	2
Sr ₂ P ₂ O ₇ :2.0 mol% Tb	2	Curve 1	0.52	0.83 ± 0.02	0.83 ± 0.04	0.81 ± 0.05	1.1 × 10 ¹⁰	2
		Curve 2	0.52	0.51 ± 0.02	0.51 ± 0.03	0.53 ± 0.02	7.3 × 10 ⁶	2
	4	Curve 1	0.52	0.84 ± 0.03	0.90 ± 0.03	0.87 ± 0.04	1.5 × 10 ¹⁰	2
		Curve 2	0.52	0.53 ± 0.03	0.52 ± 0.03	0.58 ± 0.03	9.7 × 10 ⁶	2
	6	Curve 1	0.52	0.83 ± 0.03	0.88 ± 0.03	0.87 ± 0.04	1.4 × 10 ¹¹	2
		Curve 2	0.52	0.53 ± 0.04	0.52 ± 0.04	0.55 ± 0.03	3.5 × 10 ⁷	2
Sr ₂ P ₂ O ₇ :2.5 mol% Tb	2	Curve 1	0.52	0.82 ± 0.04	0.83 ± 0.02	0.81 ± 0.02	2.9 × 10 ¹⁰	2
		Curve 2	0.52	0.56 ± 0.02	0.55 ± 0.03	0.51 ± 0.03	2.1 × 10 ⁶	2
	4	Curve 1	0.52	0.88 ± 0.03	0.90 ± 0.02	0.89 ± 0.04	4.1 × 10 ¹⁰	2
		Curve 2	0.52	0.58 ± 0.04	0.57 ± 0.04	0.56 ± 0.03	1.2 × 10 ⁷	2
	6	Curve 1	0.52	0.87 ± 0.03	0.86 ± 0.04	0.88 ± 0.04	3.2 × 10 ¹¹	2
		Curve 2	0.52	0.51 ± 0.03	0.54 ± 0.03	0.52 ± 0.03	5.5 × 10 ⁷	2
Sr ₂ P ₂ O ₇ :5.0 mol% Tb	2	Curve 1	0.52	0.86 ± 0.04	0.85 ± 0.03	0.88 ± 0.04	5.3 × 10 ¹⁰	2
		Curve 2	–	–	–	–	–	–
	4	Curve 1	0.52	0.85 ± 0.02	0.89 ± 0.02	0.87 ± 0.03	6.5 × 10 ¹⁰	2
		Curve 2	0.52	0.55 ± 0.02	0.54 ± 0.03	0.57 ± 0.02	2.8 × 10 ⁷	2
	6	Curve 1	0.52	0.84 ± 0.03	0.88 ± 0.04	0.86 ± 0.04	4.9 × 10 ¹¹	2
		Curve 2	–	–	–	–	–	–

orthorhombic structure which remains unchanged with various Tb³⁺ concentrations. The results of PL and TL studies reveal that the luminescence properties increase with doping Tb³⁺ concentration. PL studies reveal that α -Sr₂P₂O₇ doped with 5.0 mol% Tb³⁺ shows excellent green emission for a given excitation, and this material has potential to be used as a green luminescent material for display systems in solid state lighting applications. TL analyses of glow curve reveal that the TL glow curve has

two peaks analogous to traps created within band structure of host because of Tb³⁺ doping. The calculated parameters of the glow curve imply that it is of second-order kinetic. The activation energy (E_a) and frequency factor (s) are about 0.8–0.9 eV and 1×10^9 – $1 \times 10^{11} \text{ s}^{-1}$ for the curve with maximum temperature of around 420 K, respectively, and 0.5–0.6 eV and 1×10^6 – $1 \times 10^7 \text{ s}^{-1}$ for the curve with maximum temperature of 525 K. TL parameters suggest phosphor as a good TL material.

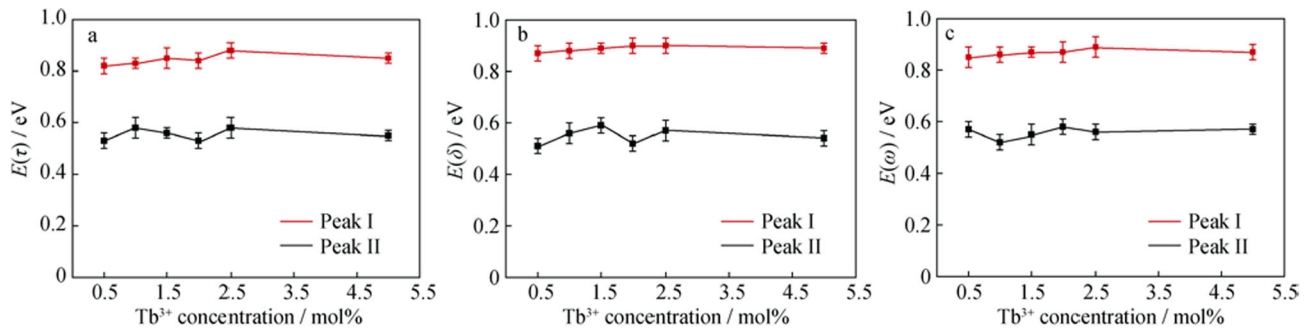


Fig. 6 Discrepancy of activation energy of Tb³⁺-doped α -Sr₂P₂O₇ with different doping concentrations at heating rate of 4 K·s⁻¹: **a** $E(\tau)$, **b** $E(\delta)$, and **c** $E(\omega)$

References

- [1] Yazici AN, Seyyidoglu S, Toktamis H, Yilmaz A. Thermoluminescent properties of Sr₂P₂O₇ doped with copper and some rare earth elements. *J Lumin.* 2010;130(10):1744.
- [2] Patel NP, Srinivas M, Verma V, Modi D, Murthy KVR. Luminescence study and dosimetry approach of Ce on an α -Sr₂P₂O₇ phosphor synthesized by a high-temperature combustion method. *J Biol Chem Lumin.* 2015;30(4):472.
- [3] Patel NP, Srinivas M, Verma V, Modi D, Murthy KVR. Synthesis and thermoluminescence dosimetry application of Dy³⁺ activated Sr₂P₂O₇. *Int J ChemTech Res.* 2014;6(3):1708.
- [4] Ma CG, Zheng W, Jin LG, Dong LM. Fluorescence and preparation of Sr₂(P₂O₇):Ce, Tb phosphate by co-precipitation method. *Rare Met.* 2013;32(4):420.
- [5] Natarajan V, Bhide MK, Dhobale AR, Godbole SV, Seshagiri TK, Page AG, Lu CH. Photoluminescence, thermally stimulated luminescence and electron paramagnetic resonance of europium-ion doped strontium pyrophosphate. *Mater Res Bull.* 2004;39(13):2065.
- [6] Henning AH, Michael D, Brohmer MC. Coactivation of α -Sr(PO₃)₂ and SrM(P₂O₇) (M = Zn, Sr) with Eu²⁺ and Mn²⁺. *Chem Mater.* 2007;19(25):6358.
- [7] Kohale RL, Dhoble SJ. Eu²⁺ luminescence in SrCaP₂O₇ pyrophosphate phosphor. *J Biol Chem Lumin.* 2013;28(5):656.
- [8] Xu M, Wang L, Jia D, Zhao H. Tuning the color emission of Sr₂P₂O₇:Tb³⁺, Eu³⁺ phosphors based on energy transfer. *J Am Ceram Soc.* 2015;98(5):1536.
- [9] Hao Z, Zhang J, Zhang X, Lu S, Luo Y, Ren X, Wang X. Phase dependent photoluminescence and energy transfer in Ca₂P₂O₇:Eu²⁺, Mn²⁺ phosphors for white LEDs. *J Lumin.* 2008;128(5–6):941.
- [10] Ye S, Liu ZS, Wang JG, Jing XP. Luminescent properties of Sr₂P₂O₇:Eu, Mn phosphor under near UV excitation. *Mater Res Bull.* 2008;43(5):1057.
- [11] Chen R. Glow curves with general order kinetics. *J Electrochem Soc.* 1969;116(9):1254.
- [12] McKeever SWS. Thermoluminescence of Solids. In: Cahn RW, Davis EA, Ward IM, editors. Cambridge: Cambridge University Press; 1985. 87.
- [13] Tiwari B, Rawat NS, Desai DG, Singh SG, Tyagi M, Ratna P, Gadhari SC, Kulkarni MS. Thermoluminescence studies on Cu-doped Li₂B₄O₇ single crystals. *J Lumin.* 2010;130(11):2076.
- [14] Xua M, Wang L, Liu L, Jia D, Sheng R. Influence of Gd³⁺ doping on the luminescent of Sr₂P₂O₇:Eu³⁺ orange-red phosphors. *J Lumin.* 2014;146:475.
- [15] Pang R, Li C, Shi L, Su Q. A novel blue-emitting long-lasting pyrophosphate phosphor Sr₂P₂O₇:Eu²⁺, Y³⁺. *J Phys Chem Solids.* 2009;70(2):303.
- [16] Shannon RD. Crystal physics, diffraction, theoretical and general crystallography. *Acta Crystallogr A.* 1976;A32(5):751.
- [17] Bow JS, Liou SC, Chen SY. Structural characterization of room-temperature synthesized nano-sized b-tricalcium phosphate. *Biomaterials.* 2004;25(16):3155.
- [18] Ledent MTP. Vibrational spectra and structure of LiB²⁺PO₄ compounds with B = Sr, Ba, Pb. *J Solid State Chem.* 1978; 23(1–2):147.
- [19] Khay N, Ennaciri A, Harcharras M. Vibrational spectra of double diphosphates RbLnP₂O₇ (Ln = Dy, Ho, Y, Er, Tm, Yb). *Vib Spectrosc.* 2001;27(2):119.
- [20] Velchuri R, Vijaya Kumar B, Rama Devi V, Jaya Prakash D, Vithal M. Solid-state syntheses of rare-earth-doped Sr_{1-x}Ln_{2x/3}MgP₂O₇ (Ln = Gd, Eu, Dy, Sm, Pr, and Nd; x = 0.05) by metathesis reactions and their spectroscopic characterization. *Spectrosc Lett.* 2011;44(4):258.
- [21] McKeever SWS, Moscovitch M, Townsend PD. Thermoluminescent Dosimetry Materials: Properties and Uses. Ashford: Nuclear Technology Publishing; 1995. 63.
- [22] Lepphoto MA, Ntwaeaborwa OM, Pitalea SS, Swart HC, Botha JR, Mothudi BM. Synthesis and characterization of BaAl₂O₄:Eu²⁺ co-doped with different rare earth ions. *Phys B Condens Matter.* 2012;407(10):1603.
- [23] Tanoria OA, Melendrea R, Monteroa MP, Casta-nedab B, Chernova V, Yenc WM, Barboza-Flores M. Persistent luminescence dosimetric properties of UV-irradiated SrAl₂O₄:Eu²⁺, Dy³⁺ phosphor. *J Lumin.* 2008;128(1):173.